

Supplementary Material

High resolution Air Quality simulation over the Himalayas, a case study in Bhutan

Bertrand Bessagnet¹, Narayan Thapa², Dikra Prasad Bajgai², Ravi Sahu², Arshini Saikia², Arineh Cholakian¹, Laurent Menut¹, Guillaume Siour³, Tenzin Wangchuk⁴, Monica Crippa⁵, and Kamala Gurung²

¹Laboratoire de Météorologie Dynamique (LMD), École Polytechnique, IPSL Research University, Ecole Normale Supérieure, Université Paris-Saclay, Sorbonne Universités, UPMC Université Paris 06, CNRS, Route de Saclay, 91128 Palaiseau, France

²International Centre for Integrated Mountain Development (ICIMOD), Kathmandu, Nepal

³Univ Paris Est Creteil and Université Paris Cité, CNRS, LISA, F-94010 Créteil, France

⁴Jigme Singye Wangchuck School of Law, Paro, Bhutan

⁵European Commission, Joint Research Centre, Ispra, Italy

Correspondence: Bertrand Bessagnet (bertrand.bessagnet@lmd.ipsl.fr)

List of Figures

Figure S1	Nested domains for our study. The domains are perfectly nested and based on the $0.01^\circ \times 0.01^\circ$ emission database grid (in blue) developed for the study	4
Figure S2	Timeseries of observations in Thimphu	5
Figure S3	Timeseries of observed meteorological data in Haa on February-March 2025	6
Figure S4	Diurnal cycle of winds in Thimphu based on local time (UTC+6) data from February 1 st to March 9 th , 2025. Low winds are observed at night mainly coming from West/South-West along the slope (mountain breeze regime). The winds get stronger during the day turning to South/South-East along the valley.	7
Figure S5	Averaged diurnal cycles for the main air pollutant concentrations and meteorological variables. Comparison between observations and model results at the three spatial resolutions	8
Figure S6	Daily timeseries of air pollutant concentrations at Thimphu Air Quality station. Comparison between observations and model results at the three spatial resolutions	9
Figure S7	Daily timeseries of meteorological variables at various stations. Comparison between observations and model results at the three spatial resolutions	10
Figure S8	Averaged diurnal cycles of the coarse PM fraction, relative humidity and the wind speed in Thimphu Air Quality station.	11
Figure S9	Average dominant component in the very fine fraction of PM ($PM_{0.1}$), the fine fraction of PM ($PM_{2.5}$), the coarse fraction of PM (PM_{coarse}) over the widest domain THP025 (left) and THP001 (right) in March 2025. Macro species are named as CARB (BC and primary OM), OPPM (other mineral primary anthropogenic species), DUST (mineral desert dust), SALT (sum of sodium and chloride), SOA (Secondary Organic Aerosol) and SIA (Secondary Inorganic Aerosol as the sum of nitrate, sulfate and ammonium). Suffix <i>h</i> mention when the dominant species concentration is at least twice the second most important component.	12
Figure S10	VIIRS (Visible Infrared Imaging Radiometer Suite) Fire and Thermal Anomalies from the NASA worldview focused in Paro and Haa districts: https://worldview.earthdata.nasa.gov : 6 March 2025 (top), 18 March 2025 (bottom left), 30 March 2025 (bottom right).	13
Figure S11	Average Aerosol Optical Depth for March 2025 from MODIS (from 0 (white) to 1 (red)), source: NASA at https://neo.gsfc.nasa.gov . Special thanks and acknowledgments go to David Herring, Jesse Allen, Eva Borbas, Jacques Descloires, Gene Feldman, Chelle Gentemann, Mark Gray, Goran Halusa, Jackie Kendall, Norman Kuring, Rebecca Lindsey, Chris Lynnes, Alex McClung, Vipool Rathod, Bill Ridgway, Holli Riebeek, Jeff Schmaltz, Michon Scott, Rob Simon, Allan Smith, Reto Stockli, Ross Swick, Stephanie Schollaert Uz, Tom Whittaker and Wenli Yang for generously sharing their time, expertise, imagery, and data. Very special appreciation goes to Vince Salomonson and Michael King for their initial support and encouragement and Steve Platnick, EOS Project Scientist, for his continuing support.	14

Figure S12 Impact of fires on Nitrate, Sulfate, NO₂ and O₃ concentrations over the THP025 domain. Average concentration decrease without fire emissions over all domains (difference NOFI - CTRL) from the 17 to 31 March. The contour lines are the reduction in % (of the CTRL reference case concentration) 15

List of Tables

Table S1	WRF namelist	16
Table S2	CHIMERE namelist: main parameters	21
Table S3	List of EDGAR categories and correspondence made between annual and monthly dataset. The monthly profiles per pollutant and macro-sectors are determined from the monthly dataset and applied to the annual dataset.	25

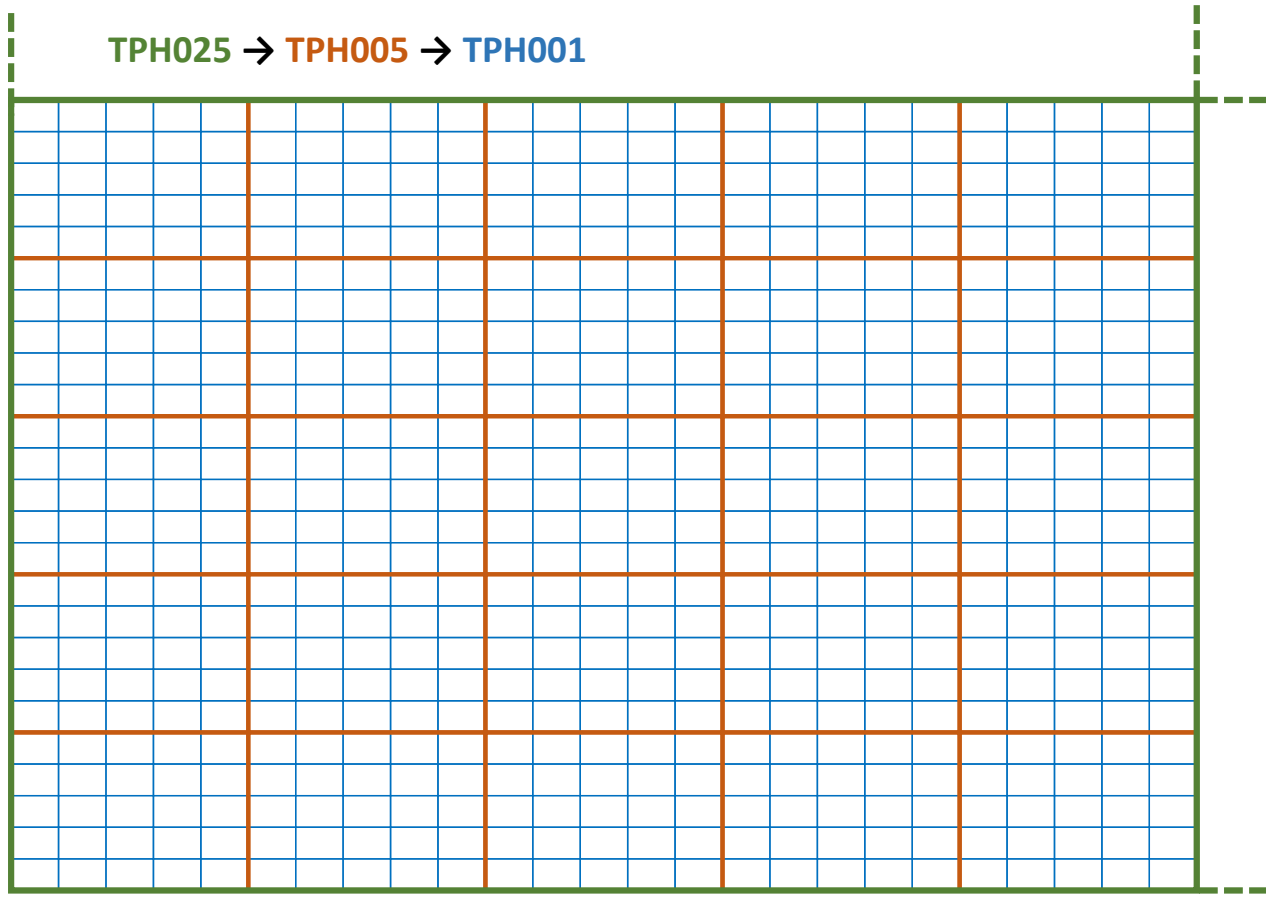


Figure S 1. Nested domains for our study. The domains are perfectly nested and based on the $0.01^\circ \times 0.01^\circ$ emission database grid (in blue) developed for the study

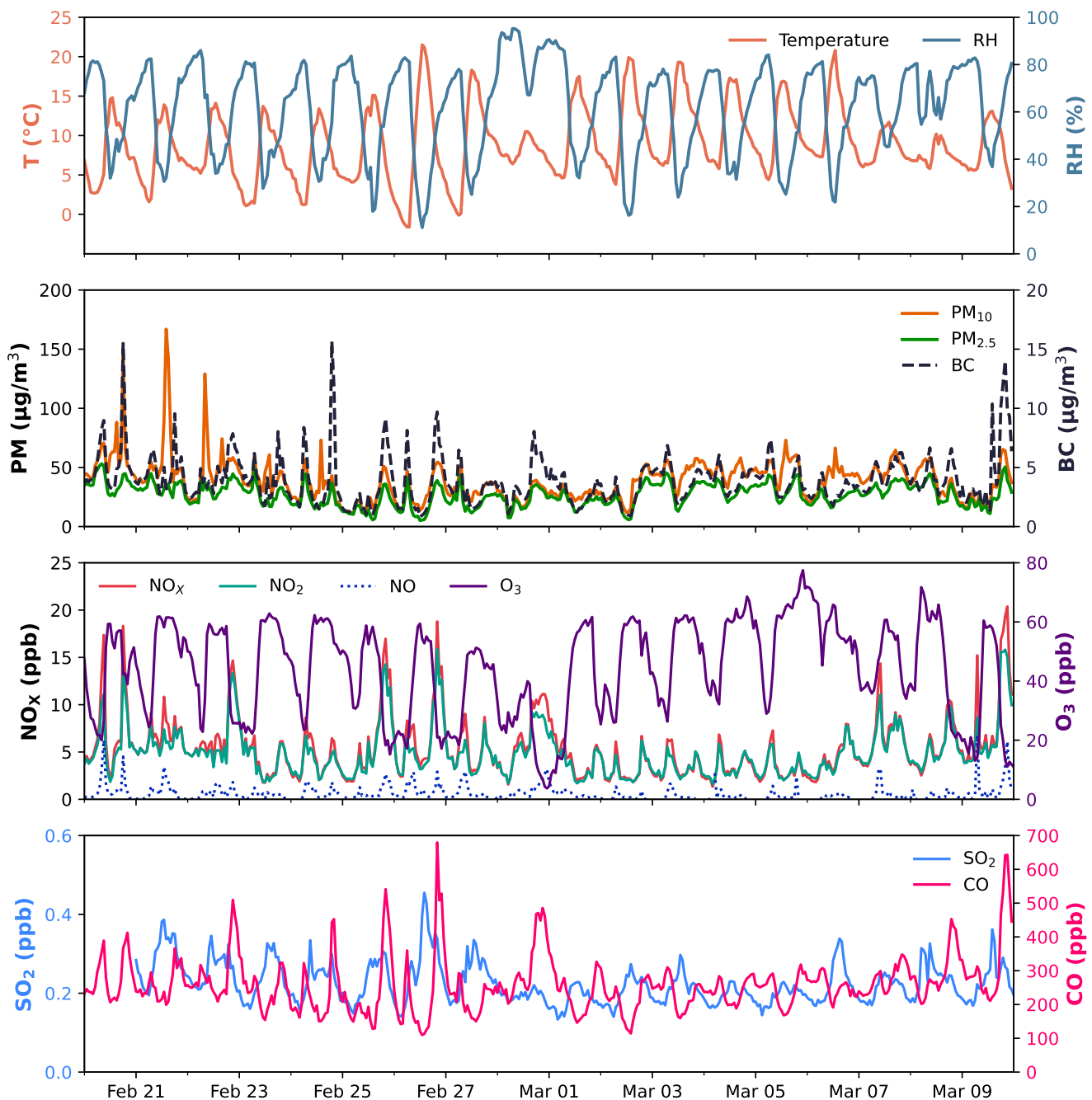


Figure S 2. Timeseries of observations in Thimphu

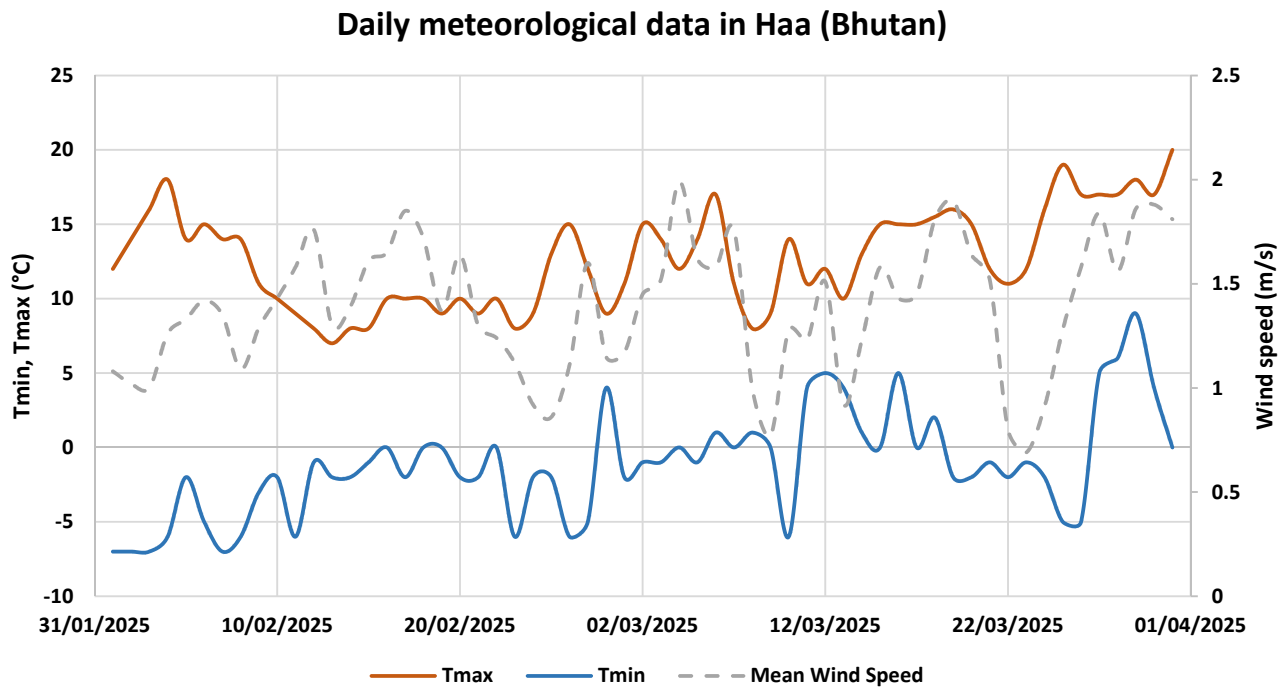


Figure S 3. Timeseries of observed meteorological data in Haa on February-March 2025

Diurnal cycle of wind speed and direction in Thimphu (Bhutan)

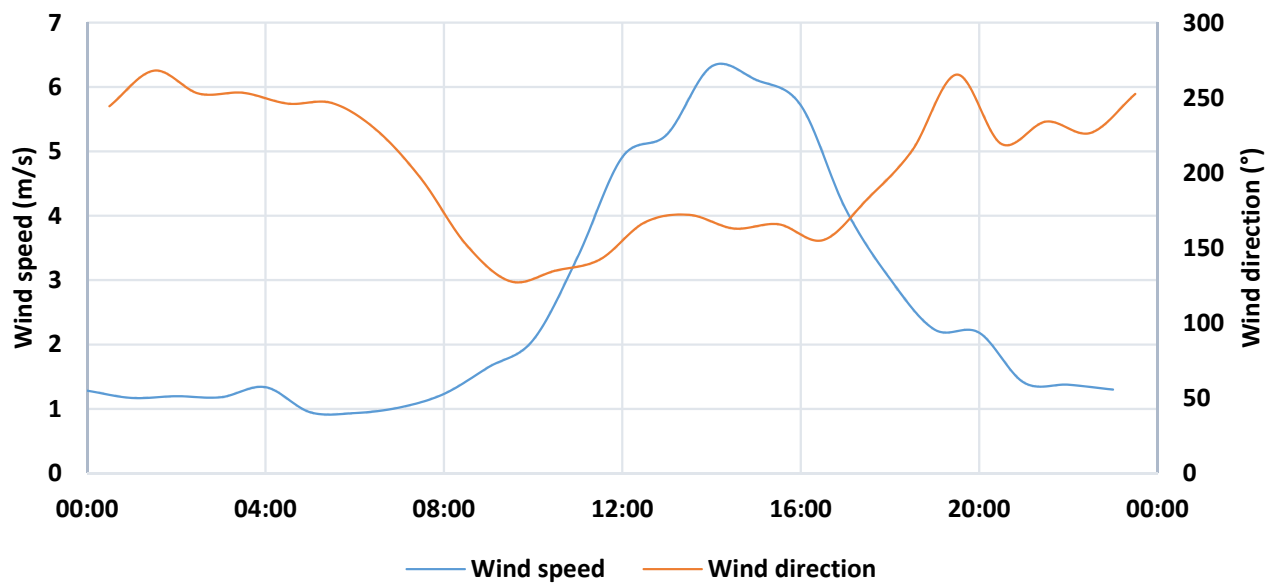


Figure S 4. Diurnal cycle of winds in Thimphu based on local time (UTC+6) data from February 1st to March 9th, 2025. Low winds are observed at night mainly coming from West/South-West along the slope (mountain breeze regime). The winds get stronger during the day turning to South/South-East along the valley.

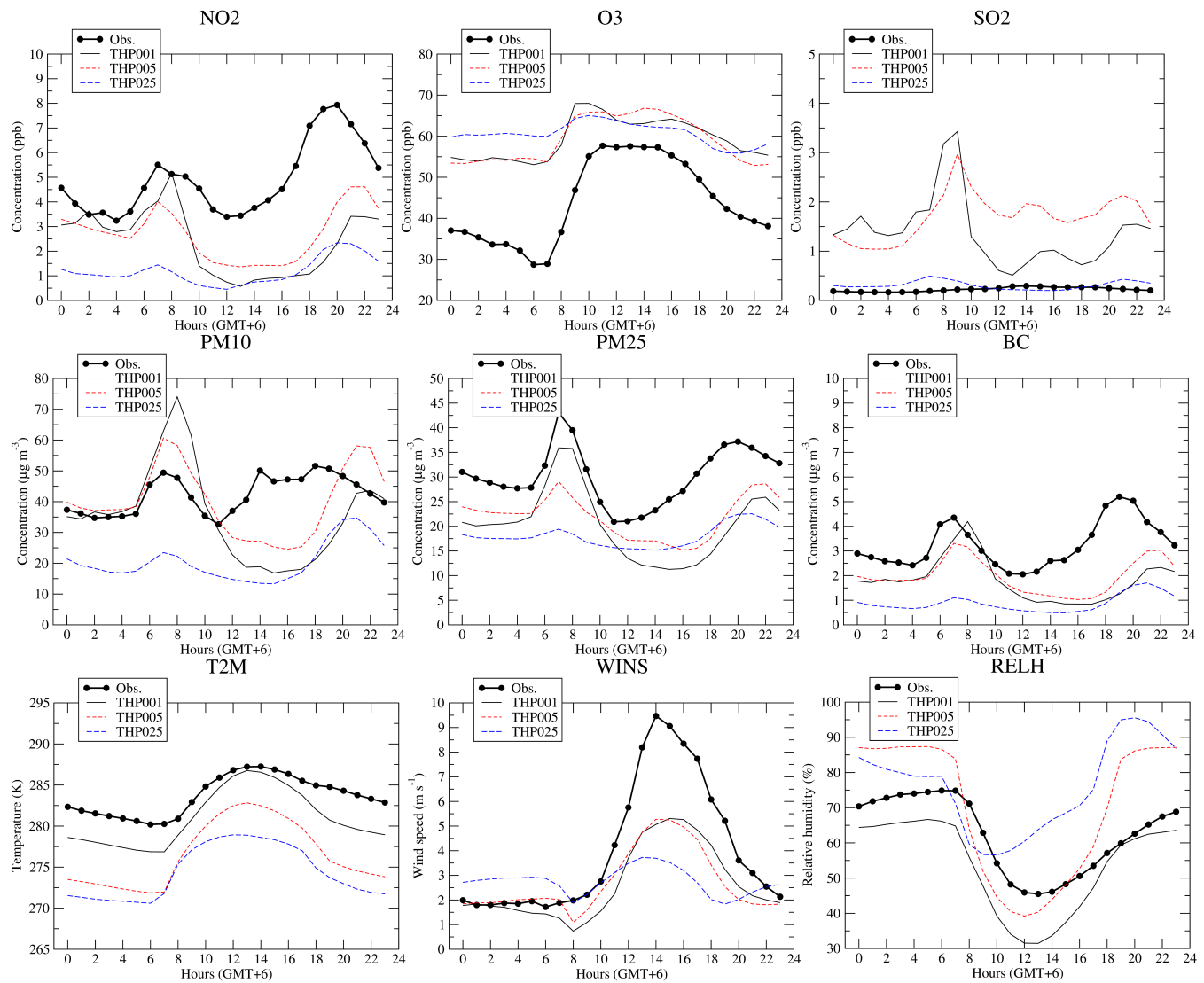


Figure S 5. Averaged diurnal cycles for the main air pollutant concentrations and meteorological variables. Comparison between observations and model results at the three spatial resolutions

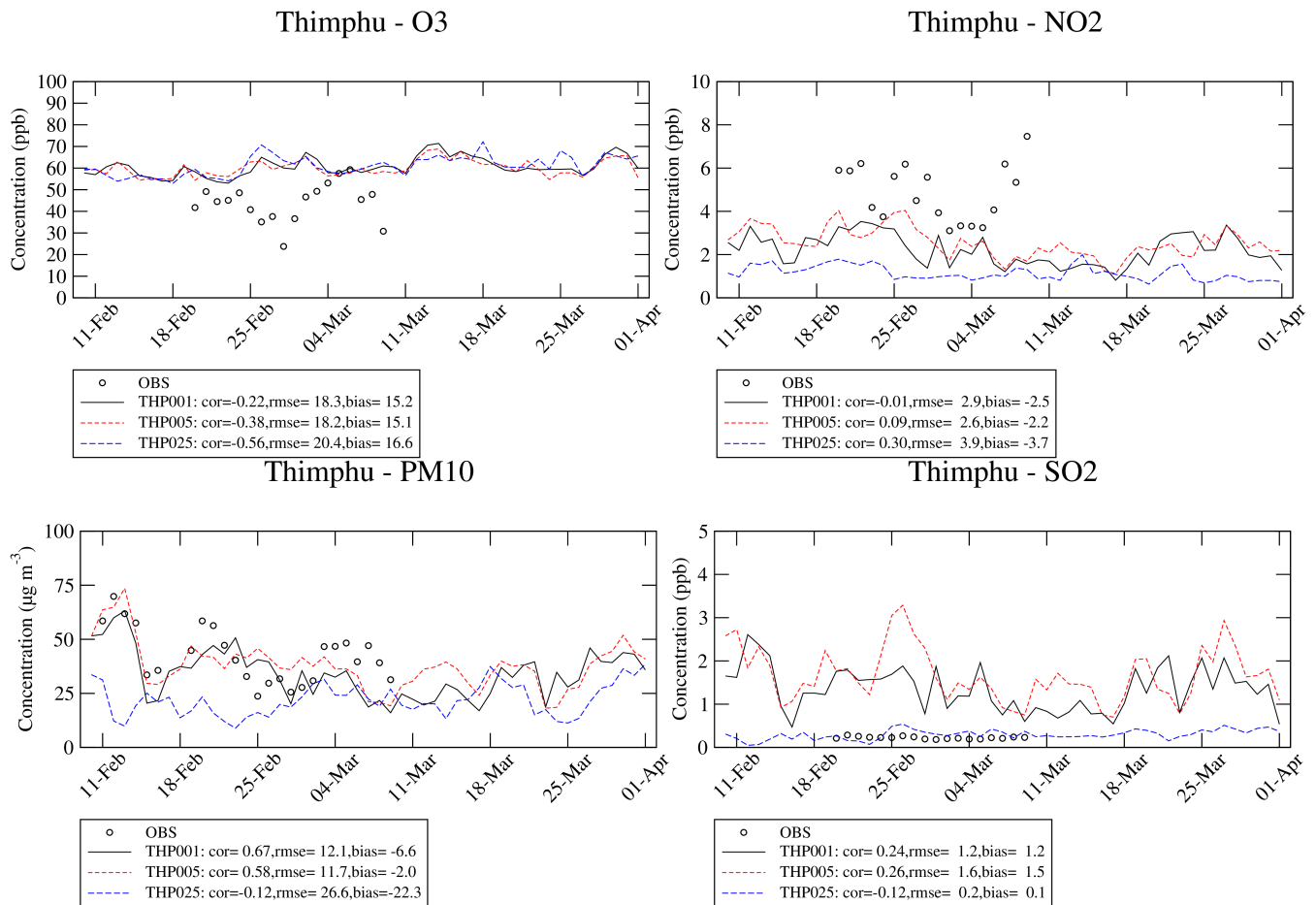


Figure S 6. Daily timeseries of air pollutant concentrations at Thimphu Air Quality station. Comparison between observations and model results at the three spatial resolutions

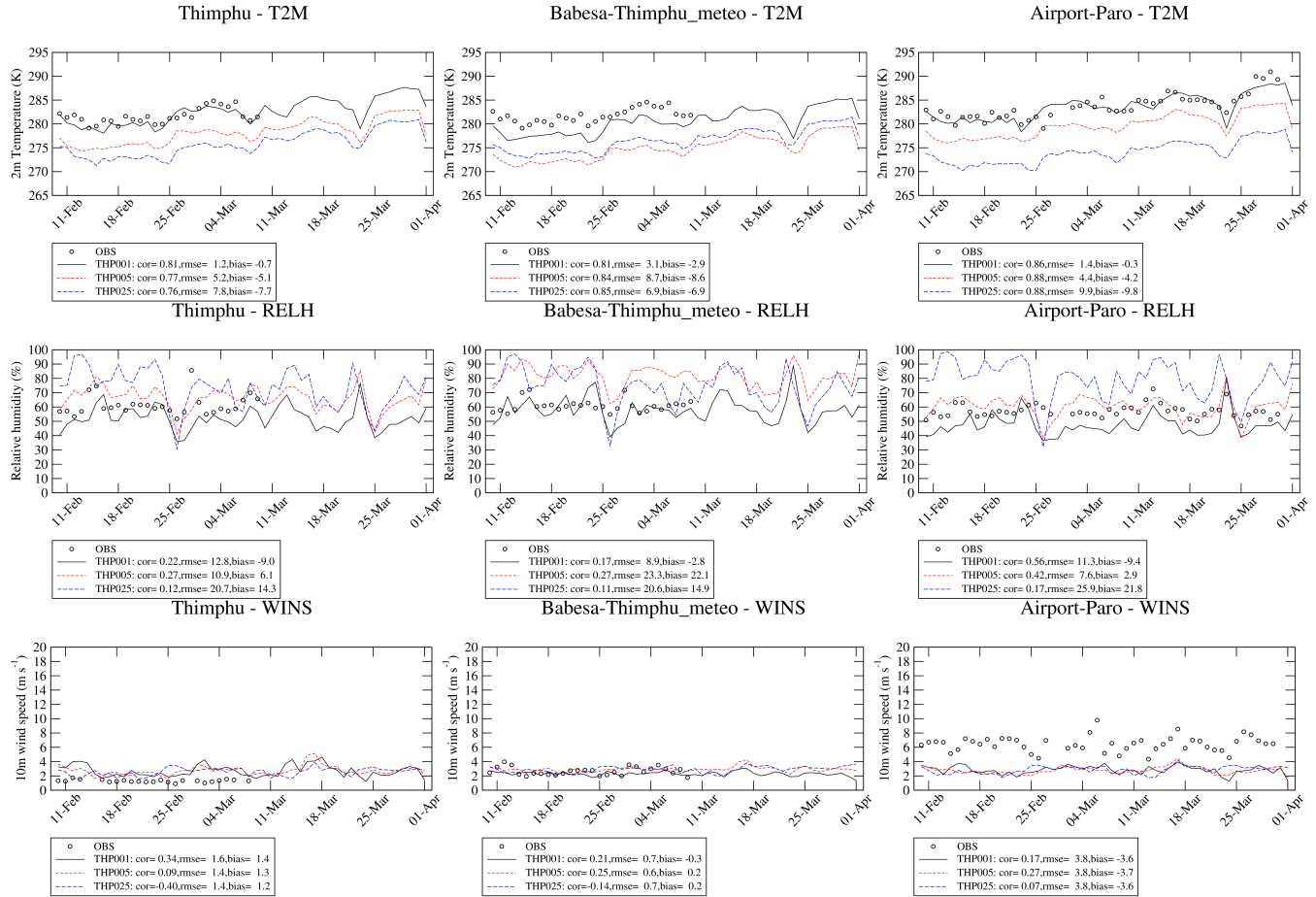


Figure S 7. Daily timeseries of meteorological variables at various stations. Comparison between observations and model results at the three spatial resolutions

Thimphu

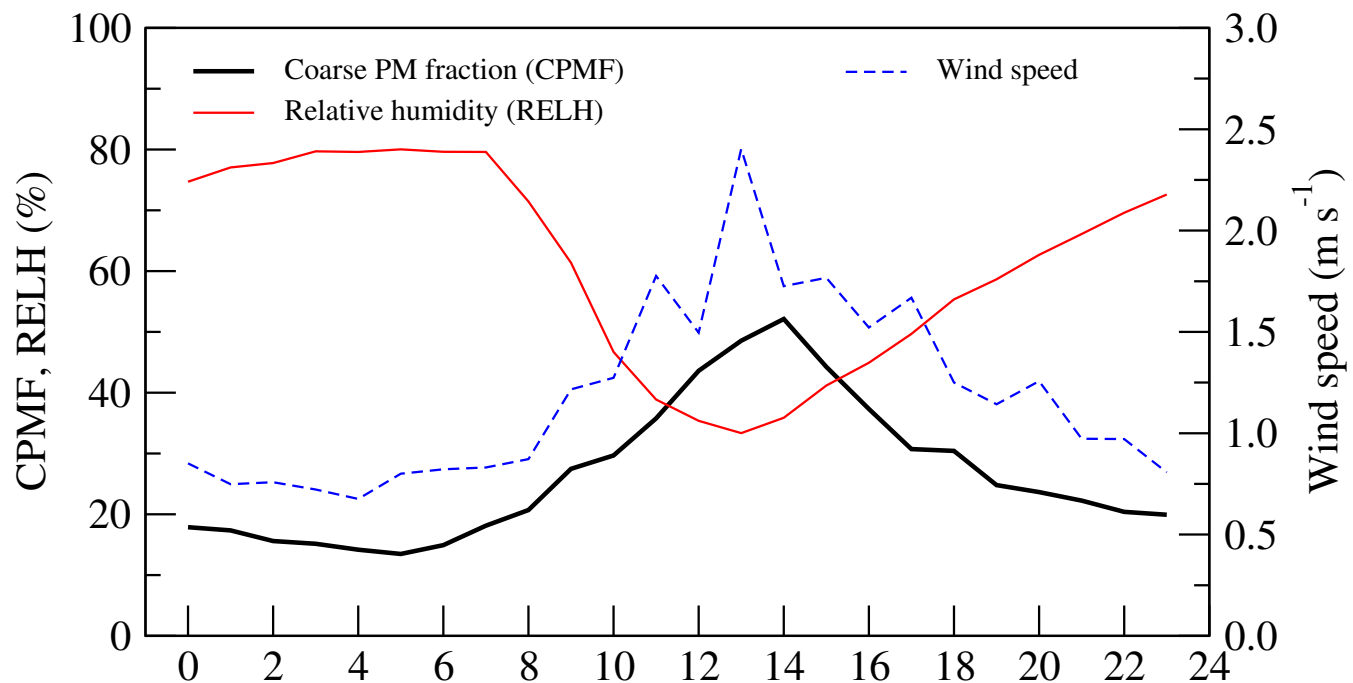


Figure S 8. Averaged diurnal cycles of the coarse PM fraction, relative humidity and the wind speed in Thimphu Air Quality station.

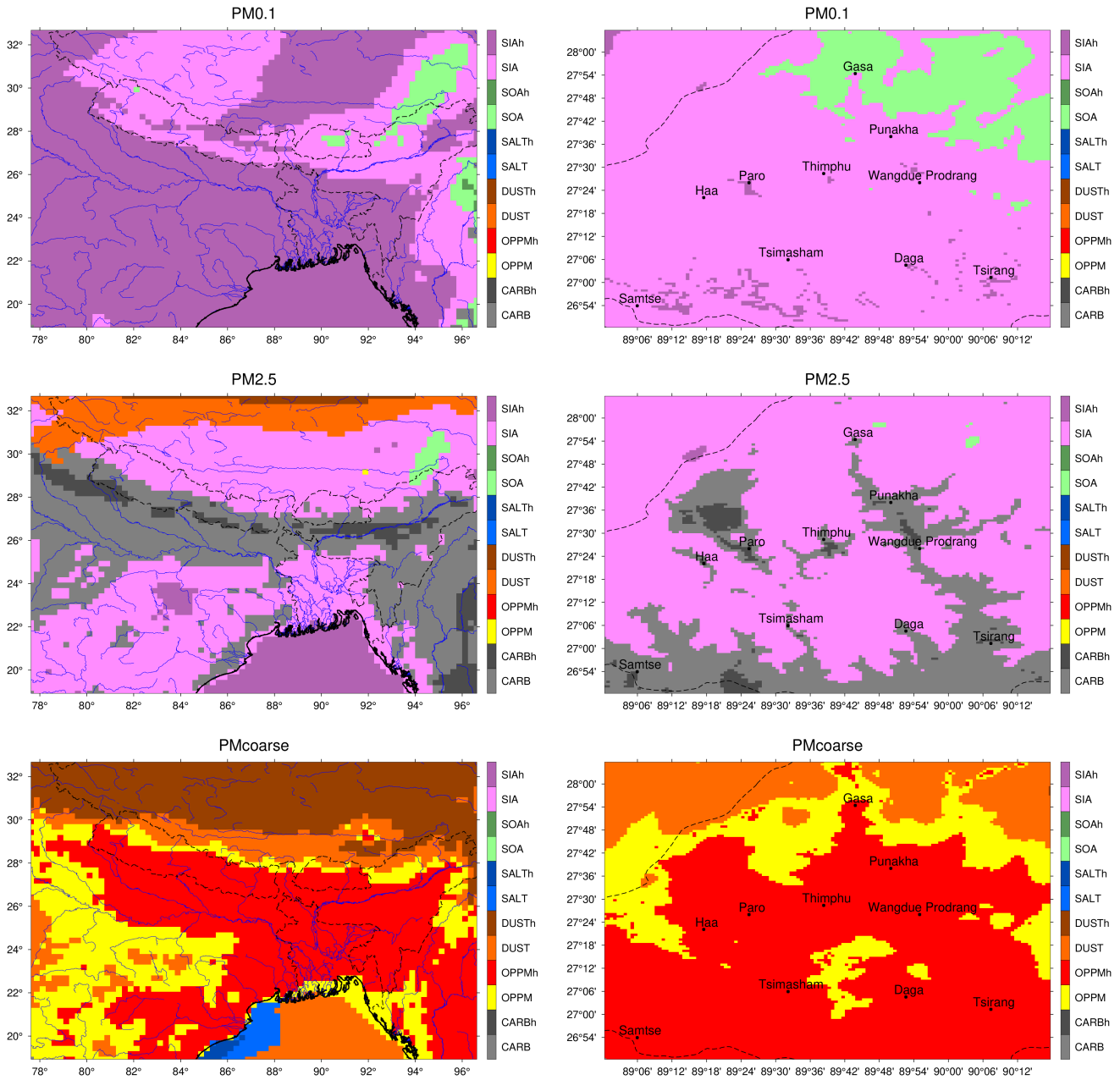


Figure S 9. Average dominant component in the very fine fraction of PM (PM_{0.1}), the fine fraction of PM (PM_{2.5}), the coarse fraction of PM (PM_{coarse}) over the widest domain THP025 (left) and THP001 (right) in March 2025. Macro species are named as CARB (BC and primary OM), OPPM (other mineral primary anthropogenic species), DUST (mineral desert dust), SALT (sum of sodium and chloride), SOA (Secondary Organic Aerosol) and SIA (Secondary Inorganic Aerosol as the sum of nitrate, sulfate and ammonium). Suffix *h* mention when the dominant species concentration is at least twice the second most important component.

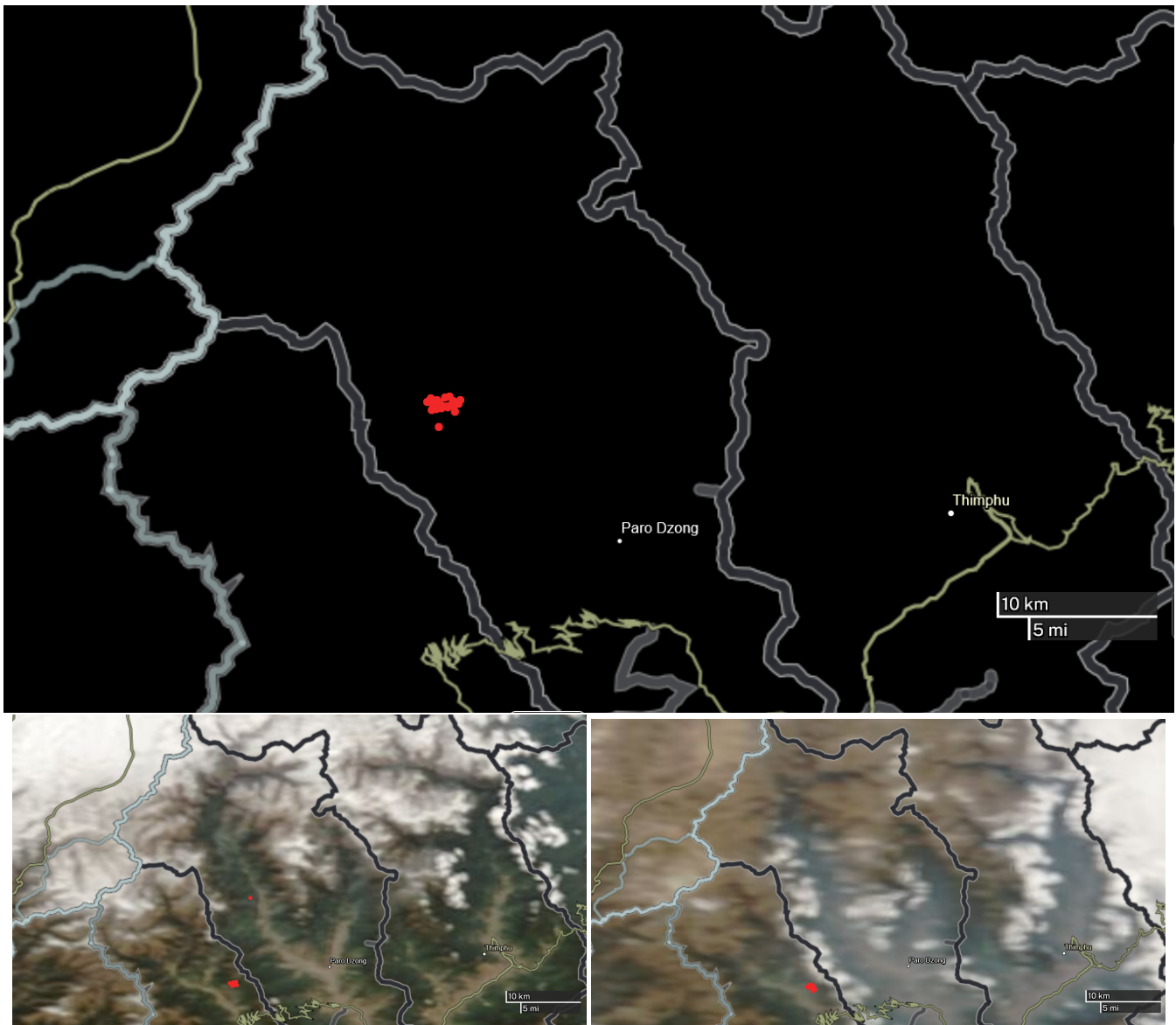


Figure S 10. VIIRS (Visible Infrared Imaging Radiometer Suite) Fire and Thermal Anomalies from the NASA worldview focused in Paro and Haa districts: <https://worldview.earthdata.nasa.gov>: 6 March 2025 (top), 18 March 2025 (bottom left), 30 March 2025 (bottom right).

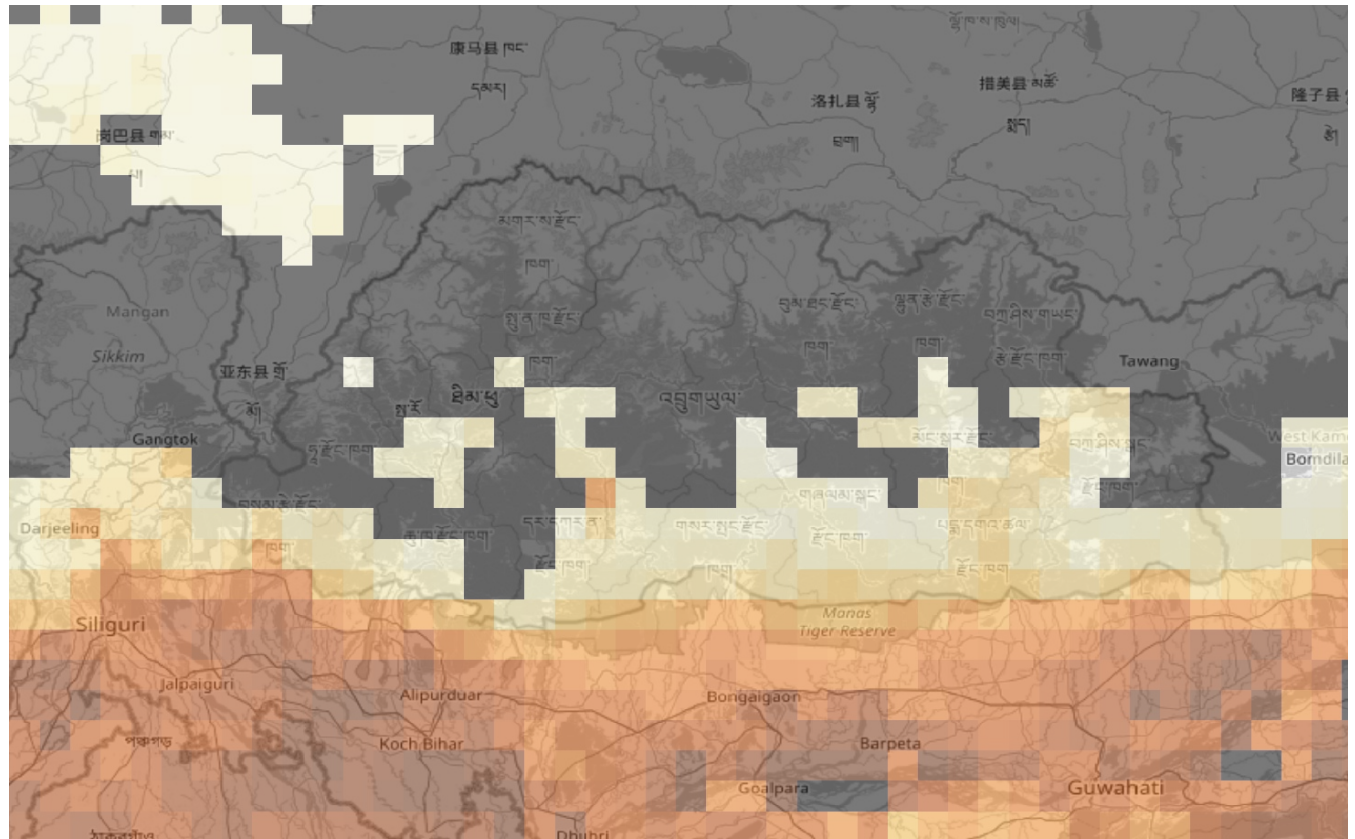


Figure S 11. Average Aerosol Optical Depth for March 2025 from MODIS (from 0 (white) to 1 (red)), source: NASA at <https://neo.gsfc.nasa.gov>. Special thanks and acknowledgments go to David Herring, Jesse Allen, Eva Borbas, Jacques Descloures, Gene Feldman, Chelle Gentemann, Mark Gray, Goran Halusa, Jackie Kendall, Norman Kuring, Rebecca Lindsey, Chris Lynnes, Alex McClung, Vipool Rathod, Bill Ridgway, Holli Riebeek, Jeff Schmaltz, Michon Scott, Rob Simmon, Allan Smith, Reto Stockli, Ross Swick, Stephanie Schollaert Uz, Tom Whittaker and Wenli Yang for generously sharing their time, expertise, imagery, and data. Very special appreciation goes to Vince Salomonson and Michael King for their initial support and encouragement and Steve Platnick, EOS Project Scientist, for his continuing support.

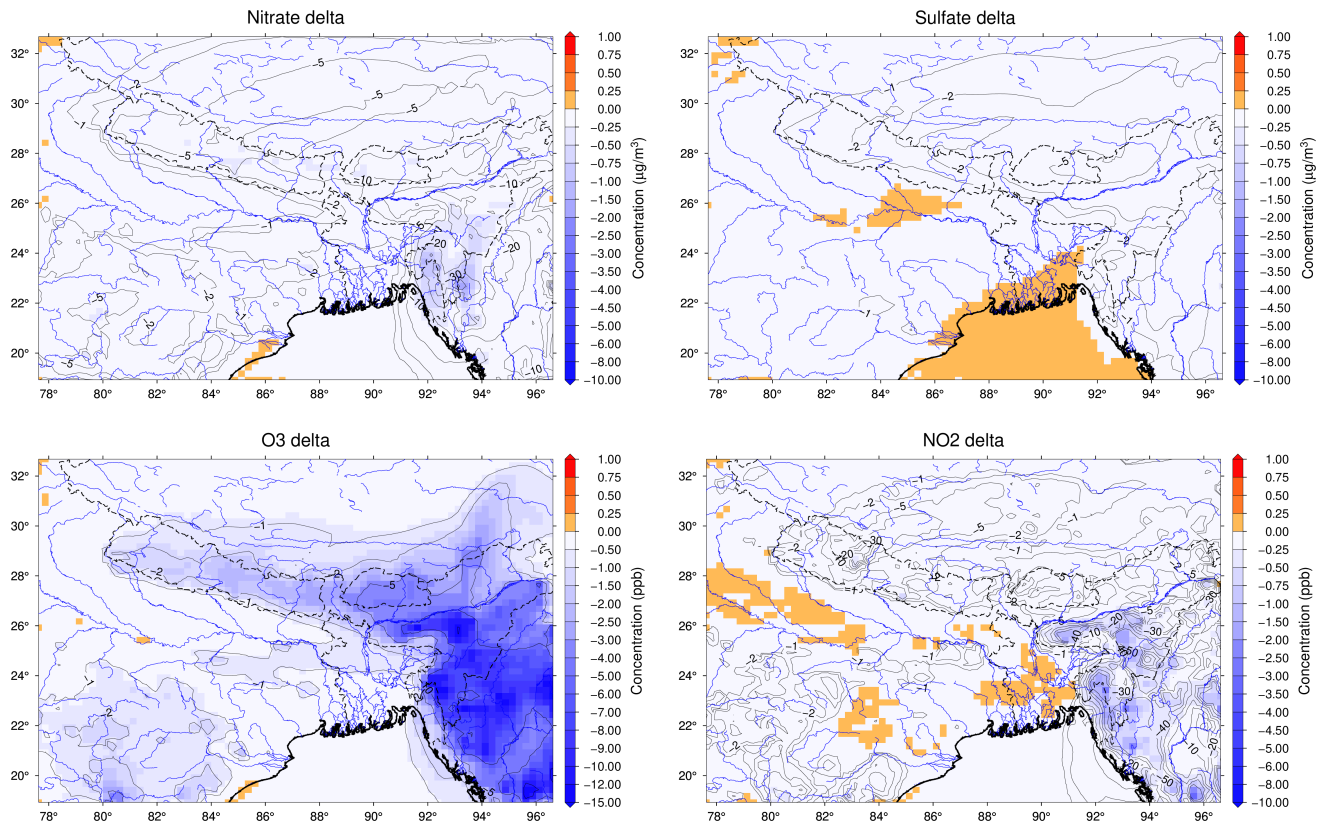


Figure S 12. Impact of fires on Nitrate, Sulfate, NO₂ and O₃ concentrations over the THP025 domain. Average concentration decrease without fire emissions over all domains (difference NOFI - CTRL) from the 17 to 31 March. The contour lines are the reduction in % (of the CTRL reference case concentration)

Table S 1: WRF namelist

Flag	Content
time_control	
run_days	0,
run_hours	0,
run_minutes	0,
run_seconds	0,
start_year	_Y1_, _Y1_, _Y1_ ,
start_month	_M1_, _M1_, _M1_ ,
start_day	_D1_, _D1_, _D1_ ,
start_hour	_H1_, _H1_, _H1_ ,
start_minute	00, 00, 00,
start_second	00, 00, 00,
end_year	_Y2_, _Y2_, _Y2_ ,
end_month	_M2_, _M2_, _M2_ ,
end_day	_D2_, _D2_, _D2_ ,
end_hour	_H2_, _H2_, _H2_ ,
end_minute	00, 00, 00,
end_second	00, 00, 00,
interval_seconds	_INTERVALSECOND_ ,
input_from_file	.true.,.true.,.true.,
history_interval	_DTPHYS1_, _DTPHYS2_, _DT- PHYS3_ ,
frames_per_outfile	100000, 100000, 100000,
restart	_WRFRESTART_ ,
restart_interval	1440,
io_form_history	2,
io_form_restart	2,
io_form_input	2,
io_form_boundary	2,
io_form_auxinput4	2,
debug_level	0,
use_netcdf_classic	.true.
auxinput4_inname	"wrfflowinp_d<domain>" ,

auxinput4_interval	360,360,360,
auxinput5_inname	"wrflowinp_d<domain>",
auxinput5_interval	6,
io_form_auxinput2	2,
write_hist_at_0h_RST	.true.,
adjust_output_times	.true.,
domains	
use_adaptive_time_step	.false.,
step_to_output_time	.true.,
starting_time_step	-1,
time_step_fract_num	0,
time_step_fract_den	1,
time_step	_Timestep_,
max_dom	_MAXDOM_,
s_we	1, 1, 1,
e_we	_E_WE1_, _E_WE2_, _E_WE3_,
s_sn	1, 1, 1,
e_sn	_E_SN1_, _E_SN2_, _E_SN3_,
s_vert	1, 1, 1,
e_vert	46, 46, 46,
p_top_requested	3000,
num_metgrid_levels	_NUMLEVELS_,
num_metgrid_soil_levels	4,
dx	_DX1_, _DX2_, _DX3_,
dy	_DY1_, _DY2_, _DY3_,
grid_id	1, 2, 3,
parent_id	0, 1, 2,
i_parent_start	_IPARSTART1_, _IPARSTART2_, _IPARSTART3_,
j_parent_start	_JPARSTART1_, _JPARSTART2_, _JPARSTART3_,
parent_grid_ratio	1, _GRIDRATIO2_, _GRIDRATIO3_,
parent_time_step_ratio	1, _GRIDRATIO2_, _GRIDRATIO3_,
feedback	_FEEDBACK_,
smooth_option	0,

vert_refine_fact	1,
sfcp_to_sfcp	.true.,
chm_sections	_CHM_SECTIONS_
eta_levels	1.0, 0.998, 0.996, 0.994, 0.991, 0.988, 0.985, 0.981, 0.976, 0.97, 0.954, 0.934, 0.909, 0.88, 0.8468087, 0.8136175, 0.7804262, 0.7472349, 0.6869155, 0.6303617, 0.5773776, 0.5277758, 0.4813772, 0.4380107, 0.3975129, 0.3597277, 0.324506, 0.2917058, 0.2611914, 0.2328334, 0.2065087, 0.1820996, 0.1594944, 0.1385863, 0.119274, 0.101737, 0.08598896, 0.0718475, 0.05914868, 0.04774535, 0.03750533, 0.02830995, 0.02005265, 0.01263772, 0.00597923, 0,
physics	
mp_physics	_cloud_mp_-, _cloud_mp_-, _cloud_mp_-
progn	0,
ra_lw_physics	4, 4, 4,
ra_sw_physics	4, 4, 4,
radt	_RADT_-, _RADT_-, _RADT_-
aer_opt	1,
alevsiz	12,
no_src_types	6,
direct_feed_chimere	_direct_feed_chimere_-,
indirect_feed_chimere	_indirect_feed_chimere_-,
sf_sfclay_physics	5, 5, 5,
sf_surface_physics	4, 4, 4,
bl_pbl_physics	5, 5, 5,
bldt	0,
cu_physics	1, 1, 1,
cugd_avedx	1,
cudt	0,
sf_urban_physics	0,

maxiens	1,
maxens	3,
maxens2	3,
maxens3	16,
ensdim	144,
isfflx	1,
ifsnow	0,
icloud	1,
surface_input_source	1,
num_soil_layers	4,
num_land_cat	_NUMLANDCAT_,
cu_rad_feedback	.true., .true.,.true.,
ysu_topdown_pblmix	0,
n_bin	_NBIN_,
sst_update	1,
topo_wind	1,
fractional_seaice	1,
fdda	
grid_fdda	2, 0, 0
gfdda_inname	"wrffdda_d<domain>",
gfdda_end_h	800000,
gfdda_interval_m	360,
fgdt	0,
if_no_pbl_nudging_uv	1,
if_no_pbl_nudging_t	1,
if_no_pbl_nudging_q	1,
if_no_pbl_nudging_ph	1,
if_zfac_ph	0,
guv	0.0003,
gt	0.0003,
gq	0.0003,
gph	0.0003,
xwavenum	_XWAVENUM1_, _XWAVENUM2_, _XWAVENUM3_,

ywavenum	_YWAVENUM1_, _YWAVENUM2_, _YWAVENUM3_,
io_form_gfdda	2,
dynamics	
w_damping	1,
diff_opt	2,
km_opt	4,
diff_6th_opt	2, 2, 2,
diff_6th_factor	0.12, 0.12, 0.12,
epssm	0.1, 0.1, 0.5,
base_temp	290.,
damp_opt	3,
zdamp	5000., 5000., 5000.,
dampcoef	0.2, 0.2, 0.2
khdif	0, 0, 0,
kvdif	0, 0, 0,
non_hydrostatic	.true., .true., .true.,
moist_adv_opt	1, 1, 1,
scalar_adv_opt	1, 1, 1,
bdy_control	
spec_bdy_width	5,
spec_zone	1,
spec_exp	0.,
relax_zone	4,
specified	.true., .false., .false.,
nested	.false., .true., .true.,
grib2	
namelist_quilt	
nio_tasks_per_group	0,
nio_groups	1,

Table S 2: CHIMERE namelist: main parameters

Flag	Content
forecast	0
nested	no,yes,yes
dom	THP025,THP005,THP001
nlevels	20
pres_topdom	200
pres_top1lev	998
nproc_chimere	100
nproc_wrf	15
nproc_xios	2
lab	COARSE1,NEST2,NEST3
clab	none,COARSE1,NEST2
sim	<i>idatestart_nhours_lab</i>
simuldir	<your path>
coarsedir	<your path>
accur	full
nsconcs	24
nsdepos	6
accurmet	medium
ilidar	0
AODPerSpecies	.false.
bigfilesdir	<your path>
landcover_dir	<your path>
geodata	<your path>
online	1
cpl_case	1
meteo	WRF
metdom	d01,d02,d03
is_diagwinw	.false.
ideepconv	1
urbancorr	0
idiagblh	0
idiagflux	0

runwrfonly	0
dgrb	<your path>
imakemeteo	1
meteo_DIR	<i>simuldir</i>
meteo_file	WRFOUTan_dom*
wrfrestart	optional
wrf_tstep_grid	6
wrfforcing	GFS
runwrfonly	0
asurfemis	1
apointemis	0
emissdir	<your path>
iuse_firemis	1
ifirevprof	1
ifire2dust	0
ifire2lai	0
ifire2drydep	0
fire_emissdir	<your path>
iusebemis	1
ilai	MOD
megan_data	<your path>/MEGAN
ip_ragweed	0
ip_birch	0
ip_grass	0
ip_alder	0
ip_olive	0
ipolresus	0
pollendir	<i>bigfilesdir/POLLEN_data</i>
iusedust	0
icuth	1
ifluxv	2
ifecan	1
iusedms	1
iusesalt	1
ilinox	1

gtrc	0
ptrc	0
iusebound	2
iuseini	2
nest_topconc	1
bcdir	<your path>
bcgas	LMDz4_INCA3_96x95x19_v2013c
bcgasdt	1
bcaer	LMDz4_INCA3_96x95x19_v2013c
bcaerdt	1
bcdust	GOCART
bcdustdt	1
mecachim	2
aero	1
nbins	10
dmin	0.01
dmax	40.0
iforcut	1
carb	1
soatyp	med
iadrydep	1
resusp	1
sgmodel	0
dtphys	5,20,20
dtchem	5,20,20
ngs	2
nsu	3
irs	1
iadv	2
iadvv	1
imethod	0
splitcfl	1
cflmax	.6.,8.,8
imakechemprep	2
istopchemprep	0

istopdom	0
chimverb	2
timeverb	0
do_clean	full

Table S 3. List of EDGAR categories and correspondence made between annual and monthly dataset. The monthly profiles per pollutant and macro-sectors are determined from the monthly dataset and applied to the annual dataset.

Monthly class	Description	Annual class
AGS	Agricultural soils	AGRICULTURE
AWB	Agricultural waste burning	AGRICULTURE
CHE	Production of chemicals	IND PROCESSES
ENE	Energy	POWER INDUSTRY
ENF	Enteric fermentation	AGRICULTURE
FFF	Fossil fuel fires	IND COMBUSTION
FOO	Food Production	IND PROCESSES
IND	Combustion in manufacturing industry	IND COMBUSTION
IRO	Iron and Steel production	IND PROCESSES
MNM	Manure Management	AGRICULTURE
NFE	Non-Ferrous metals production	IND PROCESSES
NMM	Production of non metallic minerals	IND PROCESSES
PAP	Pulp and Paper production	IND PROCESSES
PRO	Production of fuels	FUEL EXPLOITATION
PRU	Production and Use of other products	IND PROCESSES
RCO	Small scale combustion	BUILDINGS
REF	Refineries	FUEL EXPLOITATION
SOL	Solvents	FUEL EXPLOITATION
SWD	Solid Waste Disposal	WASTE
TNR	Non-road transport	TRANSPORT
TRF	Transformation industry	IND PROCESSES
TRO	Road Transport	TRANSPORT
WWT	Waste Water Treatment	WASTE
PRU_SOL	Solvents	FUEL EXPLOITATION
NEU	Non energy use of fuels	IND PROCESSES
PRO_FFF	Fuel Exploitation	FUEL EXPLOITATION
TNR_Aviation_CDS	Aviation climbing&descent	TRANSPORT
TNR_Aviation CRS	Aviation cruise	TRANSPORT
TNR_Aviation_LTO	Aviation landing&takeoff	TRANSPORT
TNR_Aviation_SPS	Aviation supersonic	TRANSPORT
TNR_Other	Railways, pipelines, off-road transport	TRANSPORT
TNR_Ship	Shipping	IND PROCESSES
FOO_PAP	Food and Paper	IND PROCESSES
SWD_LDF	Solid waste landfills	WASTE
SWD_INC	Solid waste Incineration	WASTE
REF_TRF	Oil refineries & Transformation industry	FUEL EXPLOITATION